AL-Bahir
Journal for Engineering and Pure Sciences
BJEPS

Volume 3 | Issue 2 Article 6

Using Powder Metallurgy Process to Produce Ceramic-Metal Composites

Ibrahim F. Abed
Physics, Department, College of Science, Cankiri Karatekin University, Cankiri, Turkey

Salih, Y. Darweesh
Physics, Department, College of Education Tuzkormato, Tikrit University, Tikrıt, Iraq

Recommended Citation

Abed, Ibrahim F. and Darweesh, Salih, Y. (2023) "Using Powder Metallurgy Process to Produce Ceramic-Metal Composites," *Al-Bahir*: Vol. 3: Iss. 2, Article 6.
Available at: https://doi.org/10.55810/2313-0083.1046

ORIGINAL STUDY

Using Powder Metallurgy Process to Produce Ceramic-metal Composites

Ibrahim F. Abed [a], Salih Y. Darweesh [b,*]

[a] Physics, Department, College of Science, Cankiri Karatekin University, Cankiri, Turkey
[b] Physics, Department, College of Education Tuzkormato, Tikrit University, Tikrit, Iraq

Abstract

Pressing powders and engineering materials is an innovative method for producing samples with a low cost and multiple industrial applications. In the current article, copper metal was added in different volume ratios to a ceramic material, alumina, for the purpose of improving the properties of alumina, by pressing with a hydraulic press. Where the results of the article showed that the percentage of true porosity after sintering is from (26−13)% with a copper content of (5%) to (25%). As for the apparent porosity after sintering, it decreased from (26−9)% at a copper content of (5−25)%, while the water absorption was directly proportional to the real and apparent porosity. As for the results, the Vickers hardness increased after sintering from(54−101)Kg/mm^2 at a copper content of (5−25)%. As for after heat treatment, there was a gradual increase in the resistance from (73−118)N/mm^2 at a copper content of (5−25)%. As for the synthetic results of SEM, the best consistency was at (25%) copper, and the X-ray diffraction results showed the emergence of new phases that significantly strengthen the composites and improve the mechanical and structural properties And a clear improvement during the crystalline structure, and thus we find that the appearance of the phase ($CuAlO_2$) is characterized by high durability and strength that hinders crystalline dislocations.

Keywords: Composite material, Hardness, Porosity, Copper

1. Introduction

Different shapes in powder technology can be designed by changing the shape of the molds used, as powder metallurgy has great applications in the field of cutting tools or in internal combustion engines, as well as the ease of manufacturing pistons in this way, and therefore many researchers turn to it [1,2]. The modern industrial development in the field of composite materials has led to the emergence of many advanced ceramic materials that are characterized by high durability, hardness, wear resistance, and other distinctive mechanical properties, because any manufacturing needs a reinforcing material in the composite materials, and thus the basic materials can be divided into types, including materials with a metal basis, a ceramic basis, or a polymer basis. As for the support materials, a wide range of them can be used, and some of them are in the field of nano [3]. Determining the types of reinforced materials helps greatly in predicting the physical results that can be obtained, and therefore the type of reinforcement determines the method of applying this press for any industrial work that is suitable, for example, ceramic-based materials supported by minerals are characterized by resistance to corrosion and abrasion, even in the field of renewable energy [4]. The diversity of the use of materials with metal support for various applications, including in sporting goods, moving parts, abrasive and mechanical materials, and the low cost, light weight and aesthetics have a significant impact on the type of material produced [5]. These inclusions may be continuous fibers, discontinuous particles, or thin strong threads such as silicon, and reinforcing materials include carbides such as (SiC, B_4C), nitrides such as (Si_3N_4), oxides such as (SiO_2, Al_2O_3) and some elements such as (C,

Received 22 July 2023; revised 10 August 2023; accepted 10 August 2023.
Available online 02 September 2023

* Corresponding author.
E-mail addresses: ibraheemfkhry@gmail.com (I.F. Abed), salih.younis@tu.edu.iq (S.Y. Darweesh).

https://doi.org/10.55810/2313-0083.1046

Si), and silicon carbide SiC, for example, has been widely used In mineral-based composite materials, as metal-based materials have a wide impact on industrial applications because they have results at the level of mechanical properties [6], the article aims to study the effect of adding copper as reinforcing particles with volume ratios up to (25%) on some physical properties of a system with a ceramic basis of alumina (Al_2O_3) produced by powder metallurgy technology, as well as the effect of the sintering process on these structural and mechanical properties, where the metal acts as a supportive bonding material that helps to increase and improve properties such as hardness The wear and compressive strength of the prepared models, which can be used in various industrial applications, such as their use in the manufacture of car parts and some parts of spacecraft, as well as in places that need corrosion resistance, a number of electric brushes, exchanger tubes, capacitors, and many other applications (see Table 1).

2. Raw material

The reinforced material was used of copper of Indian origin with a size of $\leq$ 44 μm manufactured by (Central Drug House) with a purity of 99.5% and a density of 8.96 g/cm^3 and a melting point of 1083 °C, while the base material was aluminum oxide (alumina) of German origin with a size of $\leq$ 63 μm from Fluka Company with a purity of 99.99% and a density of 3.95 g/cm^3 and at a melting point of 2072 °C.

3. Experimental methods

The presses resulting from the composite (Al_2O_3−%Cu) were prepared in a powdery manner and by volumetric ratios, because there is a difference in density between each of the base material and the support material. Variable support ratios were taken from copper metal, which are (5,10,15,20,25)% and added to aluminum oxide. Before starting the pressing process, the powders must be ground and mixed with each other by means of a homemade mill and they contain steel balls with a diameter of 10 mm For a period of 2 h,

Table 1. Characteristics of the X-ray diffraction tester.

voltage	**40*KV***
The current	**30mA**
scanning speed	$\frac{5^\circ}{min}$.
scanning range	$(20^\circ - 80^\circ)$
wave length	$1.54060\,A^\circ$

the mixed powders resulting from the mixing are dried in an oven for half an hour and at a temperature of 80 °C to get rid of any moisture that affects the pressing process. The pressing process of the powders is carried out by means of a hydraulic piston from the HONMAKSAN company of Turkish origin and at a pressure of 350 MPa for a time of 1 min. The samples resulting from pressing, which are called presses, suffer from weakness in the structural structure, which must be strengthened by means of a thermal oven at a high temperature of 1100 °C for a period of 2 h. Also, care must be taken to place the presses through special lids and cover them with sand and refractory clay to avoid any oxidation during the convection oven, which was of the Muffle type of Korean origin. The pistons produced from the furnace need to be cleaned with alcohol and then run with silicon carbide paper at 2000°, polished and prepared for the purpose of structural as well as physical tests. Failure to prepare and polish the samples negatively affects the results, especially the structural ones.

4. Tests used

1. Hardness Test

Vickers micro-hardness is one of the types of hardness through which the scratch resistance of the material is calculated by the metal or overlay. Vickers hardness was used because it is suitable for composites used from ceramics and metal. A diamond pyramid with a head at an angle of 136° was used with a pressure of up to 500 Kg for half a minute, after which the diameter of the resulting impact is calculated and the relationship below is applied to find out the micro-hardness [7].

$$HV = \frac{2P\sin\frac{136^\circ}{2}}{d_{av}} \quad (1)$$

Where: H_V: Hardness(Kg/mm^2), P: The load (N), d_{av}: Average Diameter(mm^2).

2. Porosity Test

The real porosity and the apparent porosity were calculated using Archimedes' rule by weighing the pistons while they were dry, and that is considered the first weight w_1, after which the pistons are immersed in distilled water for a period of 24 h, then cleaned of water sticking to their surface and weighted to represent the second weight w_2, while the third weight is done by suspending the sample through distilled water neglected weight on a sensitive scale and calculated to give w_3, the three

weights (w_1,w_2,w_3) are applied with equations Especially as in below to give the values of porosity [8–10].

$$A.P. = \frac{W_3 - W_1}{W_3 - W_2} \times 100\ \% \quad (2)$$

$$T.P. = \frac{T.D. - B.D.}{T.D.} \times 100\ \% \quad (3)$$

Where: T.P.: The percentage of total porosity, B.D.: Represents the density of the body g/cm^3,

T.D.: Represents the theoretical body density (g/cm^3).

3. Compressive Strength Test

The value of the compressive strength is calculated by means of a device that contains two jaws, each of which is flat and equal in base. The pistons are placed diagonally and a load is applied to the samples in MPa units. When the sample fails and cracks occur, the device will give the value of the resulting load. By applying the relationship below, the resistance is calculated [11].

$$\sigma_D = \frac{2F}{\pi dh} \quad (4)$$

Where: σ_D: Represents the amount of compressibility (MPa), F: The highest weight of the projector N, d: Diameter of the models in (mm) unit, h: Represents the height of the model (mm).

4. Scanning Electron Microscope

During the examination with the scanning electron microscope, electrons are used instead of light waves, and the samples are placed through a column of air and the column is emptied of air. The electronic cannon fires a high-energy beam of electrons towards a series of magnetic lenses that are designed to collect the beam in a precise place. Near the bottom of the vacuum column there is a group of scanning magnetic coils, which in turn move the focused beam of electrons over the sample to be examined back and forth, row by row, until the samples are completely covered and at the touch. The electronic beam of the surface of the sample results in the liberation of secondary electrons from the surface of the sample, and these liberated electrons are detected through a special detector that also sends a special signal to the electronic signal amplifier device, and the final image is formed of the number of electrons liberated from each point on the surface of the sample [12,13].

5. X-ray Diffraction:

The device used to examine the structures of the samples prepared by the X-ray method is (X'Pert, High, Score Plus) of Dutch origin. The tube used is type kα, (Cu), and the structural tests were carried out with X-rays at a temperature of 25 °C, as shown in Table (1) below, the characteristics of the device used for this purpose.

5. Results and discussion

1. Effect of Reinforcement Content Cu on True Porosity:

Fig. 1 gives the relationship between the real porosity and the supported copper content before

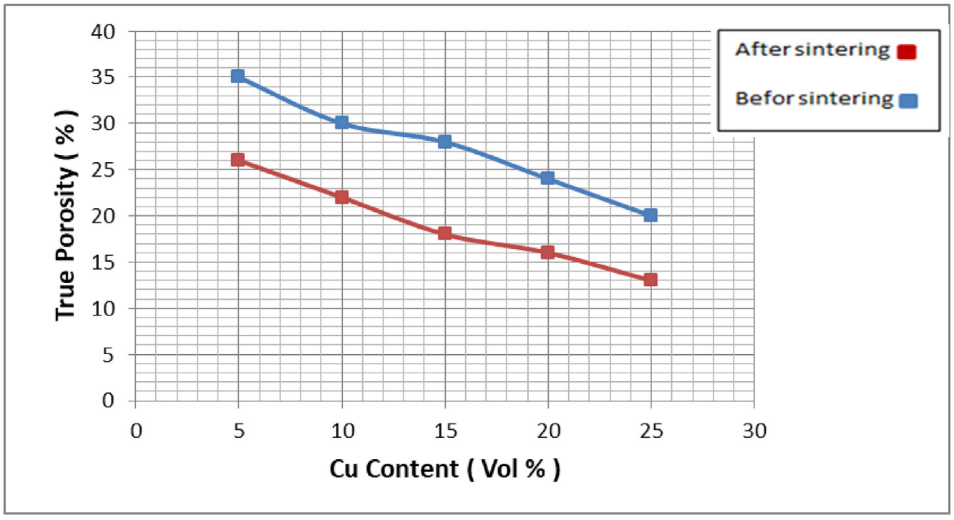

Fig. 1. Gives the relationship between Cu and true porosity before and after sintering.

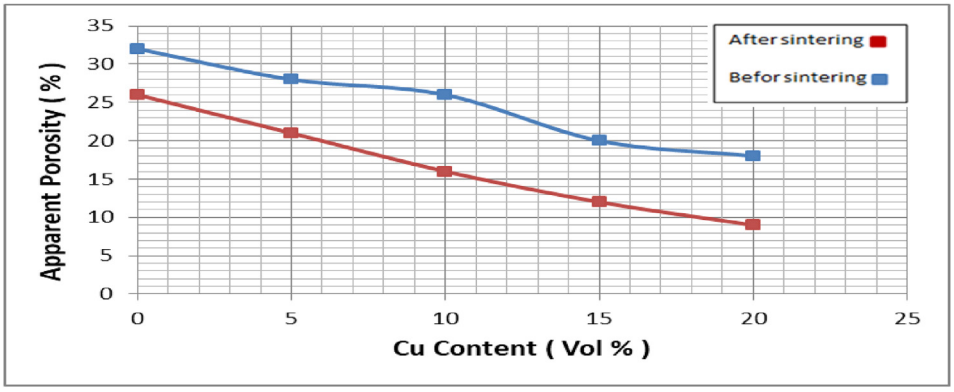

Fig. 2. The relationship between the ratio of Cu and the Apparent Porosity before and after sintering.

and after sintering, as we find that before sintering, the real porosity decreases in value from (35-25%) when reinforcing with copper from (5–25)%, but after sintering its value becomes from (13–26)% when reinforcing from (5–25)%. This decrease is due to the values of the porthole before and after the tilted Improving adhesion and reducing stresses between pistons [14,15].

2. Effect of Reinforcement Content Cu on Apparent Porosity:

Fig. 2 gives the results of mixing between the apparent porosity and the content of reinforcement with copper metal before and after sintering, and we find that repeated additions of copper metal before sintering work to reduce the porosity ratios significantly and follow the same behavior as the real porosity, and we find that the value of the apparent porosity is from % (32–18)% when cementing from(5–25)%. But after thermal treatments at 1100 °C, we notice a further decrease in the apparent porosity, and it becomes from (26–9)% when cementing from % (5–25)%. This decrease in porosity values has many reasons, the most important of which is that filling open voids is faster and larger than closed ones due to the speed of water reaching them, and thermal sintering at this high temperature has a significant effect on removing internal stresses that occur at the interfaces between the two base and supporting materials [16].

3. Effect of Reinforcement Content Cu on Hardness:

Fig. 3 gives the micro-hardness values and percentages of repeated additions of copper before and after thermal sintering processes, and we find before thermal sintering that the hardness values are low and begin to increase with each addition to reach the best of 25%, where the hardness was (44–82) Kg/mm^2 from reinforcement (5–25)%. As for the heat treatment at 1100 °C, we find that there is a significant change in the micro-hardness values of Vickers, if the values change to get the best hardness at a reinforcement rate of 25%, and thus

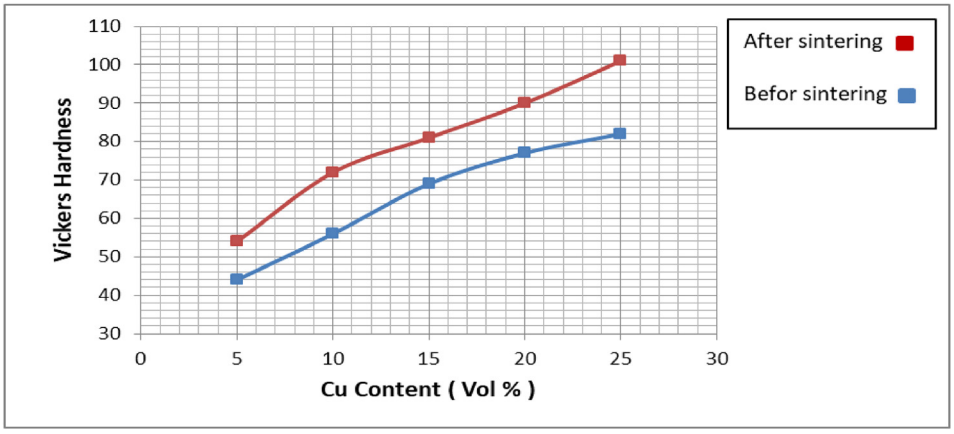

Fig. 3. The relationship between the ratio of Cu and Vickers Hardness before and after sintering.

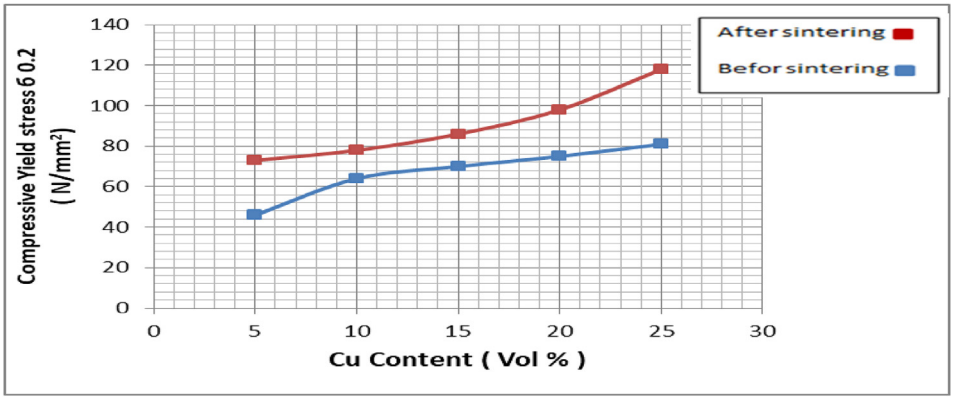

Fig. 4. The relationship between the ratio of Cu and compressive stress before and after sintering.

the hardness was from (54–101)Kg/mm^2 when reinforcing with copper from (5–25)%. The main reason for increasing the hardness values before and after sintering is cold forming, which helps to combine the two powders significantly, which contributes to a local redistribution of atoms within the alumina base material, and the effective contribution is due to the high temperature, which reaches 90% of the melting point of the reinforcing material [17].

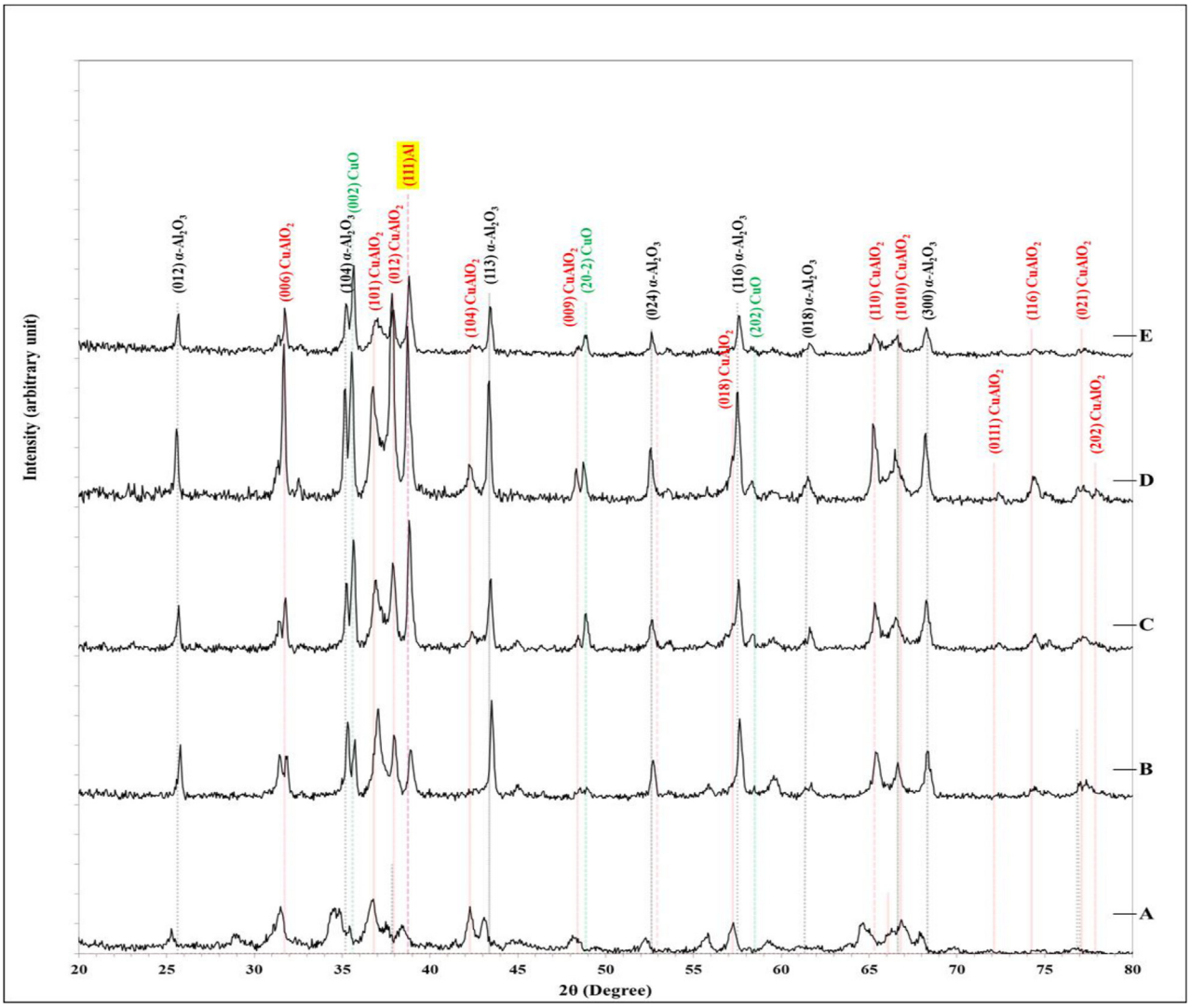

Fig. 5. X-ray diffraction of the composite (Al_2O_3–%Cu) at different percentages of copper reinforcement and after thermal sintering.

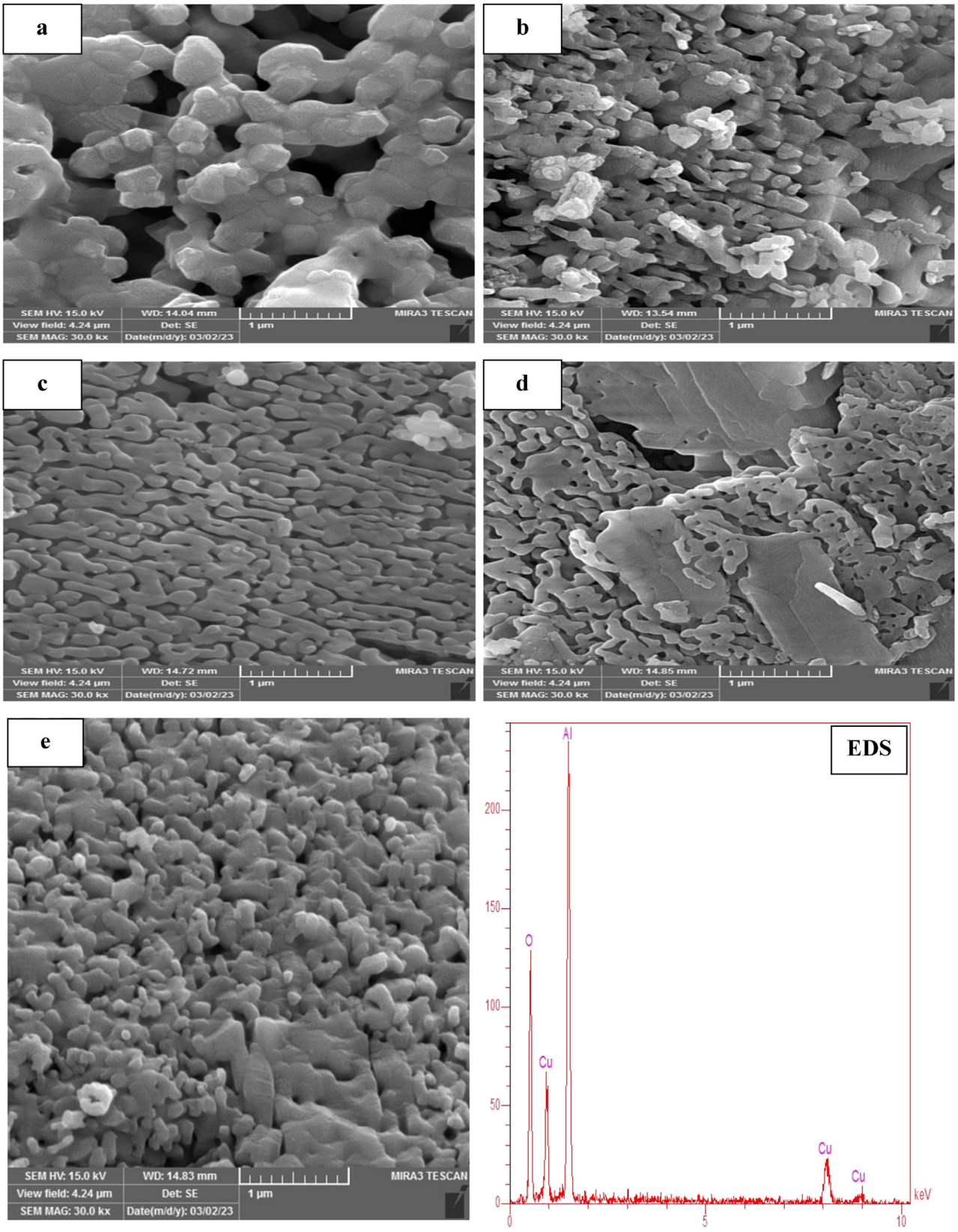

Fig. 6. Scanning Electron Microscope images of the (Al_2O_3–%Cu) after sintering with different reinforcement ratios are as follows (a-5%, b-10%, c-15%, d-20%, e–25%).

4. Effect of Reinforcement Content Cu on Compressive Strength:

We notice in Fig. 4 the direct relationship between the compressive strength of the diameter and the reinforcement with copper metal before and after sintering, and thus we find that the increase of copper before sintering greatly helps to increase the compressive strength and we find its value becomes from (46–81) N/mm^2 when cementing (5–25)%, while after high heat treatments and at 1100 °C for a period of 2 h, it contributed to raising the compressive strength values significantly to become from (73–118)N/mm^2 to (5–25)%. When observing the vast difference between the compressive strength values, especially the best percentage of reinforcement, which is 25%, we find that the difference will be approximately $37N/mm^2$, and this difference is due to several reasons, the most important of which is the sintering temperature, as well as the high-pressure formation of up to 350 MPa, which facilitates the smooth flow of copper atoms interfering between the alumina base material, and copper mainly suffers from some ductility at temperatures that help to loosen and fill the voids formed [18].

5. X-Ray Diffraction (XRD) test:

The study of research samples by means of X-rays is one of the important means to identify the nature and composition of the material used in the composite materials first and to monitor the phase changes that occur on it when changing the proportions of volumetric addition of the binder secondly. Also, the phase changes on the base material (alumina) are monitored when performing the pressing process, as well as after its thermal treatment at (1100 °C) for a period of 2 h. In Fig. 5, X-ray diffraction (XRD) was examined for the overlays and at different percentages of copper support (A = 5%, B = 10%, C = 15%, D = 20%, E = 25%), and after sintering, we notice the appearance of the base material (alumina) at the international card number (α-Al2O3, Al2O3 card No.71-1123) at Miller coefficients (012), (104) and (11). 3) and (024), (018) and (300), and this is completely compatible with the global measurement, as well as the appearance of the variable copper support material in the form of oxide (CuO) at the international card number (Monoclinic, CuO card No. 96-101-1195) and in a monoclinic crystal structure at Miller coefficients (002), (202), (2–20), and we also notice the emergence of other phases as a result Crystalline interactions, including the crystalline phase ($CuAlO_2$) at the international card number (CuAlO2, card No. 75–2361) at Miller coefficients (006), (101), (012), (104), (009), (018), (110), (1010), (116), (021), as well as the appearance of the aluminum phase separately in a cubic phase and at Miller coefficients (11). 1). And the emergence of these new phases works greatly to strengthen the complexes and improve the mechanical and structural properties and a clear improvement in the crystalline structure. Thus, we find that the appearance of the phase (CuAlO2) is characterized by high durability and strength that hinders crystalline dislocations [19].

6. Scanning Electron Microscopy and X-ray spectroscopy (EDX and SEM):

Figure (a, b, c, d, e) (6) gives scanning electron microscope images at a depth of (1 μm) and at reinforcement percentages with copper metal (5,10,15,20,25%) and after thermal sintering, and we find that the addition of the mineral support material repeatedly contributes to recrystallization and coalescence in the presence of heat. Gradually, we find that there is an improvement in the crystalline structure, especially at high addition rates, the best of which is at 25%. The consistency of the surface and the improvement of properties are mainly due to thermal sintering and cold and high-pressure forming processes that work on the overlapping of the grains with each other. The temperature at 1100 °C and a time of 2 h has a role in the distribution and filling of voids and their convergence [20]. Thus, we find that the crystalline borders between the complexes are almost hidden due to the high temperature. The results of X-ray spectroscopy (EDS) gave the most important elements. Used for copper metal and aluminum oxide, with equal distribution between the two powders, as in Fig. 6.

6. Conclusion

The important conclusion is the reinforcement of a metallic material into a ceramic material, which led to the improvement of some physical properties, such as reducing the actual and apparent porosity, as well as the mechanical properties, where the hardness increased significantly, especially when the reinforcement ratio was 25% of copper, and a clear improvement in the compressive strength of the diagonal. As for the structural properties, we find in the X-ray diffraction test a clear appearance of copper and the presence of the CuAlO2 phase, which is characterized by high hardness. Yana, but the results of X-ray spectroscopy gave the basic materials of oxygen and aluminum, which was

clearly separated from the oxygen, as well as copper.

References

[1] Angelo PC, Subramanian R, Ravisankar B. Powder metallurgy: science, technology and applications. PHI Learning Pvt. Ltd; 2022.

[2] Salih EJ, Allah SMA, Darweesh SY, Mohammed HA. Study of some of the physical variables of a metal-based system using the powder method. 1. In: Journal of physics: conference series. vol. 1999. IOP Publishing; 2021, September. p. 012068. https://doi:10.1088/1742-6596/1999/1/012068.

[3] Chryssolouris G. Manufacturing systems: theory and practice. Springer Science & Business Media; 2013.

[4] Darweesh SY, Ali AM, Khodair ZT, Majeed ZN. The effect of some physical and mechanical properties of cermet coating on petroleum pipes prepared by thermal spray method. J Fail Anal Prev 2019;19(6):1726–38. https://doi.org/10.1007/s11668-019-00772-1.

[5] Bruschi S, Cao J, Merklein M, Yanagimoto J. Forming of metal-based composite parts. CIRP Annals 2021;70(2):567–88. https://doi.org/10.1016/j.cirp.2021.05.009.

[6] Ahmed HH, Ahmed AR, Darweesh SY, Khodair ZT, Al-Jubbori MA. Processing of turbine blades using cermet composite materials. J Fail Anal Prev 2020;20(6):2111–8. https://doi.org/10.1007/s11668-020-01027-0.

[7] Salih WA, Allah SMA, Darweesh SY. Effect of spray angle on some physical properties of a ceramic system produced by thermal spraying coating. Al-Bahir J Eng Pure Sci 2023;2(2):4. https://doi.org/10.55810/2312-5721.1022.

[8] Darweesh SY, Jassim IK, Mahmood AS. Characterization of cerment composite coating Al2O3-Ni system. IOP Publishing J Phys Conf 2019, September;1294(No. 2):022011. https://doi.org/10.1088/1742-6596/1294/2/022011.

[9] Ibrahim NM. Effect of different additions of nano-zirconia on some structural and mechanical properties of (Ni-SiC) composite. Al-Bahir J Eng Pure Sci 2023;2(2):3. https://doi.org/10.55810/2312-5721.1020.

[10] Odhiambo JG, Li W, Zhao Y, Li C. Porosity and its significance in plasma-sprayed coatings. Coatings 2019;9(7):460. https://doi.org/10.3390/coatings9070460.

[11] Tjaronge MW, Irfan UR. Porosity, pore size and compressive strength of self-compacting concrete using sea water. Procedia Eng 2015;125:832–7. https://doi.org/10.1016/j.proeng.2015.11.045.

[12] Wheeler JM, Michler J. Elevated temperature, nano-mechanical testing in situ in the scanning electron microscope. Rev Sci Instrum 2013;84(4). https://doi.org/10.1063/1.4795829.

[13] Polat S, Sun Y, Çevik E, Colijn H, Turan ME. Investigation of wear and corrosion behavior of graphene nanoplatelet-coated B4C reinforced Al–Si matrix semi-ceramic hybrid composites. J Compos Mater 2019;53(25):3549–65. https://doi.org/10.1177/0021998319842297.

[14] Jana P, Ray S, Goldar D, Kota N, Kar SK, Roy S. Study of the elastic properties of porous copper fabricated via the lost carbonate sintering process. Mater Sci Eng, A 2022;836:142713. https://doi.org/10.1016/j.msea.2022.142713.

[15] Nosewicz S, Jurczak G, Wejrzanowski T, Ibrahim SH, Grabias A, Węglewski W, et al. Thermal conductivity analysis of porous NiAl materials manufactured by spark plasma sintering: experimental studies and modelling. Int J Heat Mass Tran 2022;194:123070. https://doi.org/10.1016/j.ijheatmasstransfer.2022.123070.

[16] Taha MA, El-zaidia MM, Zaki MZ, Abomostafa HM. Influence of nano-hybrid reinforcements on the improvement strength, thermal expansion and wear properties of Cu–SiC–Fly ash nanocomposites prepared by powder metallurgy. ECS J Solid State Sci Technol 2023;12(3):033011. https://doi.org/10.1149/2162-8777/acc5af.

[17] Darweesh SY, Ali AM, Khodair ZT, Majeed ZN. The effect of some physical and mechanical properties of cermet coating on petroleum pipes prepared by thermal spray method. J Fail Anal Prev 2019;19(6):1726–38. https://doi.org/10.1007/s11668-019-00772-1. .

[18] Celebi Efe G, Yener T, Altinsoy I, Ipek M, Zeytin S, Bindal C. The effect of sintering temperature on some properties of of CU–SiC composite ", sakarya university , engineering faculty , department of metallurgy and materials engineering , esentepe campus, 54187 sakarya , Turkey. J Alloys Compd 2011;509:6036–42. https://doi.org/10.1016/j.jallcom.2011.02.170.

[19] Li D, Fang X, Deng Z, Zhou S, Tao R, Dong W, et al. Electrical, optical and structural properties of CuCrO2 films prepared by pulsed laser deposition. J Phys Appl Phys 2007;40(16):4910. https://doi.org/10.1088/0022-3727/40/16/023.

[20] Gol MSG, Malti A, Akhlaghi F. Effect of WC nanoparticles content on the microstructure, hardness and tribological properties of Al-WC nanocomposites produced by flake powder metallurgy. Mater Chem Phys 2023;296:127252. https://doi.org/10.1016/j.matchemphys.2022.127252.